DOI 10.2478/ama-2023-0006

A FLYWHEEL-BASED REGENERATIVE BRAKING SYSTEM FOR RAILWAY VEHICLES

Jacek JACKIEWICZ*

*Faculty of Mechatronics, Kazimierz Wielki University, ul. Kopernika 1, 85-074 Bydgoszcz, Poland

jacek.jackiewicz@ukw.edu.pl

received 25 June 2022, revised 30 October 2022, accepted 7 November 2022

Abstract: Regenerative braking is a technique that employs electric motors to convert the dynamic mechanical energy from the motor's spinning rotor and any attached loads into electricity. However, such a type of regenerative braking can only slow but not stop the vehicle because there is too little energy to excite the motor acting as a generator at low speeds. Therefore, this paper presents a unique flywheel-based regenerative braking system for railway vehicles. This system is supposed to meet high safety and comfort expectations in all operating conditions. The braking action control of this system should allow braking of empty or loaded vehicles according to load, the anti-blockage braking action of wheels and prevent wheel-slide during braking or wheel slip during acceleration. The new regenerative braking system under development, like any kinetic energy recovery system, requires the application of continuously variable transmission. The essence of the new solution is to design and build this type of variable transmission using only one planetary gear controlled through the powertrain control module for an electric motor cooperating concurrently. This paper describes complete modelling and simulation realisation on a closed-loop servomotor drive, which cooperates with the variable transmission of the regenerative braking system based on the Scilab/Xcos environment.

Key words: railway brakes, flywheel, regenerative braking system

1. INTRODUCTION

Various railway brakes [1] are used on vehicles of railway trains to enable the deceleration of vehicles and control of acceleration of train cars going down a slope. However, when a train is parked, they are used to keep its carriages immobile. Basic systems of railway brakes can be classified as follows: pneumatic, electric, hydraulic and mechanical. All of these systems can have various designs and structural arrangements.

Suburban trains should provide a short travel time between stations. The high acceleration of the train leaving the station and then a quick reduction of its speed before the next station caused by its braking ensure such a requirement. Therefore, operating at speeds no higher than 180 km/h, the suburban trains have increased numbers of driven wheels or wheelsets in their configurations. In addition, such types of trains are not only equipped with standard pneumatic and electric brakes but can quite often be equipped with rail brakes and eddy current brakes. Anyway, this way of the train moving between stations is associated with substantial energy losses during braking because most brakes use friction between two surfaces pressed together to convert the kinetic energy of the moving vehicles into heat, commonly.

This kinetic energy can be reclaimed and stored in a reusable manner by regenerative braking systems [2]. Increasingly more modern railway vehicles with electric drive systems have regenerative braking systems to not only capture but also apply this available form of power. During braking, due to the principle of reversibility of electrical machines, electric vehicles use their traction motors to convert kinetic energy into electromagnetic energy by switching them into generator operation mode. When electric currents are produced by these dynamo-motors, the electrical energy generated from such a process can be dissipated as heat through brake grid choppers or resistors (i.e., dynamic or rheostatic braking) or can be usefully and beneficially absorbed (i.e., regenerative braking). For electric railway vehicles and systems, regenerative braking offers the capability to return this recovered braking energy to the power supply line. Besides this, the recuperated energy can be stored on the train board automatically. This method of storing energy provides distinct benefits. Namely, the consumption of stored available energy can be as independent as possible from the power supply line, and the entire system can use such energy at any convenient moment. As the application to traction systems is considered 'hybrid', the ability to self-generate power by railway vehicles allows for their less dependence on railway electrification systems.

Hybrid and plug-in hybrid drive systems have become more and more frequent for diesel-electric multiple unit regional railway vehicles [3]. When considering the design of these vehicles, they are similar to locomotives with diesel engines or gas turbines. A significant difference is that hybrid vehicles have additional electric motors besides diesel or gas turbine power units. Electric energy generated in these vehicles can be stored in electric rechargeable batteries, supercapacitors or flywheels. The charging of these components can occur during running at the idle speed of the diesel generator or gas turbine and, moreover, braking when the kinetic energy of train vehicles is transformed into electric power.

Rechargeable batteries are usually used for electrical energy storage through a reversible chemical reaction, which allows the charge to be stored again after the battery has been drained. They can be made from different combinations of electrode

materials and electrolytes. However, despite significant investments in research, around the world, for improving batteries, their use has some drawbacks. They are heavy concerning the amount of energy stored per unit mass (i.e., energy density), and their manufacturing is very costly [4]. Most importantly, their utility characteristics can significantly vary with changes in the ambient temperature of operation, which means the operation of hybrid systems equipped with batteries can be unpredictable, both in scorching heat and cold climates. In those climatic conditions, for electric batteries, it is necessary to create advanced systems for maintaining temperatures in their predetermined operating range. It entails an additional cost due to supplementary energy usage.

Aside from the technology of electric rechargeable battery packs, alternate main methods of energy storage captured via regenerative braking are the technology of supercapacitor arrays (which store potential energy depending on their state of electric charging), the technology of rotating flywheels (which store kinetic energy in the form of angular momentum) as well as compressed fluid energy storage systems. The methods of storing energy built on supercapacitors and rotating flywheels perform very reasonably and are less susceptible than electric batteries to the influence of temperature. Supercapacitors can be charged very quickly, and, by their number of cycles of charging and discharging, they have a leading position at the current time. However, supercapacitors have a shortcoming concerning their low specific energy and the limited efficiency time because of linearly reducing their voltage as power is drawn. In turn, the batteries hold their voltage during the discharging period. In the applications used so far, the rotating flywheels have a good enough ability to store energy and a virtually unlimited number of charge cycles. Comparing them with supercapacitors and batteries in terms of size, weight and operation characteristics, they are inferior. Tungsten heavy alloys (WHAs), based on W-Ni-Cu and W-Ni-Fe, belong to a group of two-phase composites [5]. Due to their advantageous combinations of high density, strength and ductility WHAs can be used as basic materials for rotors of flywheels. Moreover, penetrators in all cannon-fired kinetic energy projectiles are made of WHAs and, more often, depleted uranium (DU) alloys, U-3/4Ti, as well. Note the chemical symbol, W, of the rare metal tungsten comes from its old Swedish name, wolfram.

Nowadays, flywheels offer a reliable and durable solution for storing kinetic energy. Such a storing energy method has the potential to bring significant efficiency gains and cost reductions for mass rapid transit networks [6]. The key to efficiency improvements in rail transport is to provide a local energy storage capability, which can capture and store energy produced by braking systems and deliver it on demand to reduce the power required for an accelerating train. Moreover, any flywheel-based regeneration system can stabilise the traction power system voltage by eliminating voltage sags and peaks appearing when braking energy is dissipated through brake resistors [7, 8]. Flywheel-based energy storage technology is both proven and mature. Such technology provides a low-risk and low-cost solution as well. Flywheels have a high level of reliability, durability, and availability. They can operate continuously with two-minute minimum headways of trains without compromising product life [9, 10].

The performance of a mechanical energy storage system in the form of a flywheel depends on the properties of the used drivetrain. In [11], Read compared the operation of two drive transmission options, considering the efficiency of energy recovery from the flywheel. He examined two representative drive transmission methods: (a) electric powertrain (consisting of motor/generator, power electronics, motor, and final drive) and (b) mechanical toroidal continuously variable transmission with the final drive. These drivetrains can change seamlessly through a continuous range of gear ratios. However, they operate with efficiencies that do not exceed more than 80%. Additionally, as stated by Zhang et al. [12], control is crucial to guarantee the performance of any flywheel energy storage system.

Because of the above, the primary goal of this paper is to present a new concept of a regenerative braking system based on a flywheel. At the same time, the proposed new solution is to improve the energy efficiency of the mechanical continuously variable transmission conveying the propulsion between the flywheel and the wheels of the rail vehicle. This solution requires the design of a new control system for a servo motor that should smoothly change the gear ratio between active and passive shafts of the planetary gear to maintain a constant command value for the drive torque.

2. NEW KINETIC ENERGY STORAGE SYSTEM ABOARD RAILWAY VEHICLES

Increasing the acceleration and deceleration of trains within a railway network can improve the performance of railway passenger transport. Such a requirement is particularly desirable for urban, suburban, and regional trains, which should feature relatively high acceleration and deceleration. Passenger comfort must be additionally considered when designing railway transit systems for their performance and cost-effectiveness. It should be kept in mind that with high accelerations and decelerations of railway vehicles, the risk of passengers losing their balance and falling is also increased [13]. Between two adjacent stations, any train's run can be divided into three stages: (i) starting from the station to accelerate to a stable cruise speed, (ii) running at the cruise speed for some time, and (iii) decelerating and stopping at the next station in an interval.

This work intends to create an effective regenerative braking system for self-propelled railway vehicles. Since most railway vehicles are powered by electricity supplied through overhead contact lines or diesel engines, which are turbocharging except for a few, this recuperating braking system will be appropriate for both these drive types. Moreover, this system is incorporated into all rail vehicles, which can accelerate and decelerate quickly.

However, achieving a tractive effort diagram similar to that which can be obtainable with the electric traction systems operating so far poses a problem for vehicles powered only by diesel engines. Namely, the piston engines cannot be started under load, cannot reverse rotation direction, and do not provide a constant starting tractive effort. Therefore, transmission is necessary between the diesel engine and the railway wheels. Most diesel locomotives are diesel-electric [14]. They have all the components of a series hybrid transmission to make the drive systems more flexible and environmentally friendly. For that reason, a hybrid drive system that uses an onboard flywheel-based rechargeable energy storage system is taken here as a starting point because it can be used in both electric multiple units and electro-diesel multiple units. Recovering kinetic energy via a flywheel through regenerative braking seems promising for self-propelled railway vehicles with frequent starts/stops (see [15, 16]). Such a system in railway vehicles will have a meaningful effect on

DOI 10.2478/ama-2023-0006

energy saving; it can also drive systems to become more flexible and, at the same time, environmentally friendly. However, like any kinetic energy recovery system, the new regenerative braking system requires the application of continuously variable transmission. The essence of the new solution is to design and build this type of variable transmission using only one planetary gear controlled through the powertrain control module for a FAULHABER DC servo motor with an integrated motion controller [17], cooperating concurrently.

Fig. 1 shows a schematic representation of the hybrid traction system, which combines a motor-generator (MG) power source with the new braking energy recovery system for the electric multiple-unit bogie. The energy recovery system is mainly composed of the assembly of two flywheels, the control clutch 1, the bevel gear transmission, and the clutch 2, as a coupling device. The assembly of flywheels is used for energy storage. Both of these flywheels operate in vacuum containers. The first differential transmission is utilised to change smoothly the varying gear ratio between the powertrain and assembly of two flywheels by applying theservo motor. The clutch 2 is used to control processes of engagement, release, and sliding friction of connection between the flywheel energy storage system and drive transmission of the electric multiple-unit bogie. When electric multiple units are used for braking, the clutch is engaged gradually, and the flywheels are accelerated. If the flywheels accelerate to a certain borderline degree, the clutch is disconnected, and the flywheels rotate at a high speed in the vacuum chamber.

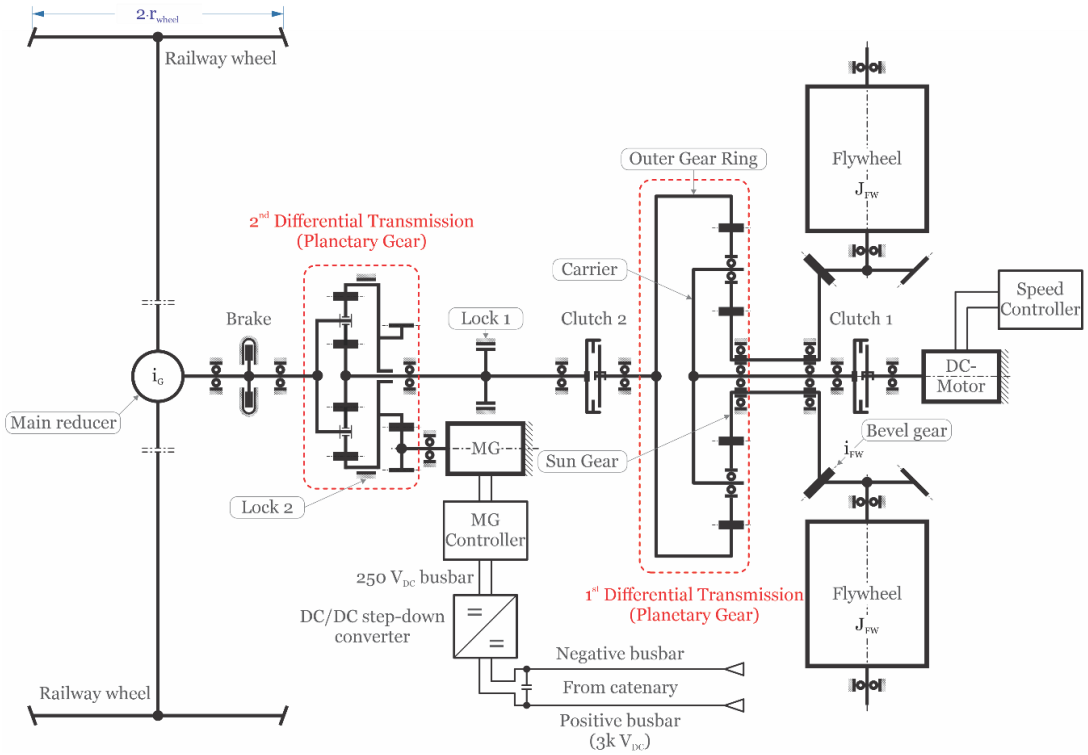

Fig. 1. Hybrid traction system, which combines motor-generator power source with mechanical flywheel energy storage system

As shown in the figure above, both differential transmissions comprise three shafts – the sun gear, the planet carrier, and the external ring gear. During regenerative braking, the three-shaft operation mode of the first planetary gear is used, in which two shafts of the outer ring and the carrier are driven, and the sun shaft is the driver. In such a case, the planetary gearset operates as a summation gear train.

Planetary gearsets are characterised by their high efficiency with the transfer of torque of large values, even in small construction spaces. They are suitable for clockwise or counter-clockwise use and in alternating, constant, and intermittent operations.

According to the analytical method of Willis [18], if the angular velocities of the two input shafts of the planetary gearset are known, the angular velocity of the output shaft can be determined by the following equation:

$$\omega_{\mathrm{C}}^{(i)} = \frac{\mathrm{N}_{\mathrm{S}}^{(i)}}{\mathrm{N}_{\mathrm{R}}^{(i)}+\mathrm{N}_{\mathrm{S}}^{(i)}}\omega_{\mathrm{S}}^{(i)} + \frac{\mathrm{N}_{\mathrm{R}}^{(i)}}{\mathrm{N}_{\mathrm{R}}^{(i)}+\mathrm{N}_{\mathrm{S}}^{(i)}}\omega_{\mathrm{R}}^{(i)}\,, \tag{1}$$

where $\omega_{\mathrm{C}}^{(i)}$, $\omega_{\mathrm{S}}^{(i)}$, and $\omega_{\mathrm{R}}^{(i)}$ are the angular velocities of the planet carrier, sun gear, and ring, respectively. In turn, $\mathrm{N}_{\mathrm{S}}^{(i)}$ and $\mathrm{N}_{\mathrm{R}}^{(i)}$ are the numbers of teeth of the sun gear and ring, respectively. In Eq. (1), the superscript, $^{(i)}$, denotes the differential transmission number.

Let's assume for a while that all gear pairs of the first differential transmission are operating with 100% efficiency. If this is the case, the total power entering and leaving the gearbox must also add up to zero [19] as follows:

$$\mathrm{M}_{\mathrm{C}}^{(i)}\omega_{\mathrm{C}}^{(i)} + \mathrm{M}_{\mathrm{S}}^{(i)}\omega_{\mathrm{S}}^{(i)} + \mathrm{M}_{\mathrm{R}}^{(i)}\omega_{\mathrm{R}}^{(i)} = 0\,, \tag{2}$$

where $\mathrm{M}_{\mathrm{C}}^{(i)}$, $\mathrm{M}_{\mathrm{S}}^{(i)}$ and $\mathrm{M}_{\mathrm{R}}^{(i)}$ determine the torque of the carrier, torque of the sun, and the torque of the ring (annulus), respectively. Moreover, to ensure invariable values of the following torques: $\mathrm{M}_{\mathrm{C}}^{(1)}$, $\mathrm{M}_{\mathrm{S}}^{(1)}$, and $\mathrm{M}_{\mathrm{R}}^{(1)}$ during deceleration or braking of the railway vehicle, the angular accelerations of the three main components of the planetary gearset (i.e., $\dot{\omega}_{\mathrm{C}}^{(1)}$, $\dot{\omega}_{\mathrm{S}}^{(1)}$,

and $\dot{\omega}_{\mathrm{R}}^{(1)}$) should also be constant. Hence, the differentiation of both sides of Eq. (2) gives

$$\mathrm{M}_{\mathrm{C}}^{(1)}\dot{\omega}_{\mathrm{C}}^{(1)} + \mathrm{M}_{\mathrm{S}}^{(1)}\dot{\omega}_{\mathrm{S}}^{(1)} + \mathrm{M}_{\mathrm{R}}^{(1)}\dot{\omega}_{\mathrm{R}}^{(1)} = 0\,. \tag{3}$$

The above condition is necessary to meet because according to Newton's Second Law of Motion in rotation, the net torque, M_{FW}, on the rotating mass with variable angular speed, $\omega_{\mathrm{FW}}(t)$, and mass moment of inertia, J_{FW}, causes it to accelerate with angular acceleration, $\varepsilon_{\mathrm{FW}} \stackrel{\mathrm{def}}{=} \dot{\omega}_{\mathrm{FW}}$:

$$M_{\mathrm{FW}} = \mathrm{J}_{\mathrm{FW}} \cdot \varepsilon_{\mathrm{FW}}\,. \tag{4}$$

As shown in Fig. 1, $\omega_{\mathrm{FW}} = \mathrm{i}_{\mathrm{FW}} \cdot \omega_{\mathrm{S}}^{(1)}$, where i_{FW} = 4.245 is the bevel gear ratio. For the first planetary gear, the teeth # of the sun is $\mathrm{N}_{\mathrm{S}}^{(1)}$ = 37, the teeth # of the ring is $\mathrm{N}_{\mathrm{R}}^{(1)}$ = 73.

To obtain greater efficiency of the drive transmission of the mechanical flywheel energy storage system proposed here than in the known solutions used so far, it is necessary that the value of the moment, $\mathrm{M}_{\mathrm{C}}^{(1)}$, should be close to zero. In this case, the flow of kinetic energy during the charging and discharging of such a variant of the so-called 'mechanical' battery will take place with very little loss.

The required value of the angular acceleration, $\varepsilon_{\mathrm{R}}^{(1)} \stackrel{\mathrm{def}}{=} \dot{\omega}_{\mathrm{R}}^{(1)}$, and the value of the torque, $\mathrm{M}_{\mathrm{R}}^{(1)}$, can be determined for given values of deceleration or acceleration of the rail vehicle and based on the analysis of its drive system. Then, considering Eqs (3) and (4), the angular acceleration, $\varepsilon_{\mathrm{S}}^{(1)} \stackrel{\mathrm{def}}{=} \dot{\omega}_{\mathrm{S}}^{(1)}$, and the torque, $\mathrm{M}_{\mathrm{S}}^{(1)}$, should be determined. Thus, using Eq. (1), the required value of the angular acceleration, $\varepsilon_{\mathrm{C}}^{(1)} \stackrel{\mathrm{def}}{=} \dot{\omega}_{\mathrm{C}}^{(1)}$, can be established, as well as the range of angular velocities of the carrier shaft from its initial to final values. Therefore, the control strategy for the FAULHABER DC servo motor to determine its desired changes of angular velocity and acceleration (or deceleration, as well) has a dramatic impact on the performance of this system, which constitutes the first differential transmission.

Similar to the first differential transmission, the second one is the speed-coupling unit, which constitutes the hybrid drivetrain.

In Fig. 1, the flywheel energy storage system supplies power to the sun gear through a clutch and transmission. The second differential transmission is used to modify the speed-torque characteristics to match the traction requirements. For this planetary gear, the teeth # of the sun is $\mathrm{N}_{\mathrm{S}}^{(2)}$ = 30, the teeth # of the ring is $\mathrm{N}_{\mathrm{R}}^{(2)}$ = 76.

The electric motor-generator supplies power to the ring gear of the second planetary gear. Lock 1 and lock 2 are used respectively to lock the sun gear and ring gear to the standstill frame of the vehicle to satisfy the different operation mode requirements. The following operation modes can be distinguished [20]:

- Hybrid traction: When lock 1 and lock 2 are released (the sun gear and ring gear can rotate), both the flywheel energy storage system and motor generator supply positive torque (positive power) to the driven wheels.
- Flywheel energy storage system alone traction or alone regenerative braking: When lock 2 locks the ring gear to the vehicle frame and lock 1 is released, only the flywheel energy storage system supplies power to the driven wheels or performs regenerative braking.
- Motor-generator alone traction: When lock 1 locks the sun gear to the vehicle frame (clutch 2 is disengaged) and lock 2 is released, only the motor-generator supplies power to the driven wheels.
- Motor-generator alone regenerative braking: When lock 1 is set in locking state, the clutch 2 is disengaged, and the motor-generator is controlled in regenerating operation (negative torque), the kinetic energy of the vehicle can be transferred by the electric system to the catenary.
- Supplying electric energy to the catenary from the flywheel energy storage system: When lock 1 and lock 2 are released, the rail vehicle brake is locked, and the flywheel energy storage system supplies positive power to the railway traction network.

The following condition, $\varepsilon_{\mathrm{R}}^{(2)} = \varepsilon_{\mathrm{S}}^{(2)} = \varepsilon_{\mathrm{C}}^{(2)}$, is assumed for the hybrid traction mode, which can be performed during acceleration or deceleration. Note that $\mathrm{M}_{\mathrm{C}}^{(2)} = \mathrm{M}_{\mathrm{wheels}}/\mathrm{i}_{\mathrm{G}}$, where $\mathrm{M}_{\mathrm{wheels}}$ is the total torque transmitted by railway wheels of one drive axle, and i_{G} = 2.39 is the final drive ratio.

3. CONCEPT OF THE CONTROL SYSTEM OF THE DC SERVO MOTOR

Correct operation of the flywheel-based regenerative braking system requires designing and building a reliable control system for the DC motorafterward. This motor can easily be speed-controlled by modifying the supply voltage providing a consistent amount of torque over its entire speed range.

The first step to designing a closed-loop control system is to identify a mathematical representation of the DC motor [21]. The DC motor can be best represented by a transfer function of a complex variable, s. The transfer function, which diagram block is shown in Fig. 2, provides a mathematical description for the DC motor that relates input voltage, $\mathcal{V}_{\mathrm{m}}(s)$, to the angular velocity of the motor shaft, $\Omega_{\mathrm{m}}(s)$. Note that the angular velocity is $\omega_{\mathrm{m}}(t) \stackrel{\mathrm{def}}{=} \dot{\theta}_{\mathrm{m}}(t)$, where θ_{m} is the angular position of the motor shaft. $\Omega_{\mathrm{m}}(s)$ and $\mathcal{V}_{\mathrm{m}}(s)$ are the signal Laplace transforms of $\omega_{\mathrm{m}}(t)$ and $v_{\mathrm{m}}(t)$, respectively.

Hence, the following equation represents the model of the DC motor:

$$\frac{\Omega_{\mathrm{m}}(s)}{\mathcal{V}_{\mathrm{m}}(s)} = \frac{\mathrm{K}_{\mathrm{m}}}{\mathrm{J}_{\mathrm{eq}}\mathrm{R}_{\mathrm{m}}s + \mathrm{K}_{\mathrm{m}}^2}\,, \tag{5}$$

where K_{m} = 0.028 Vs/rad, R_{m} = 3.3 Ω, and J_{eq} = 9.64·10-6 kg·m2 are the motor back ElectroMotive Force (EMF) constant, motor armature resistance, and equivalent moment of inertia, respectively.

The next step is to choose a control method and design a controller. The feedback system in Fig. 2 is a single-loop feedback system with a proportional-integral-derivative (PID) controller, which the controller gains (i.e., k_{P}, k_{D}, and k_{I}) should be determined to satisfy all design specifications. This closed-loop control system uses the measurement of the output and feedback of the angular motor shaft position signal, θ_{m}, to compare it with the desired input (reference or command), θ_{d}. Since the intended purpose of the control is to simultaneously determine the desired angular velocity, $\omega_{\mathrm{d}}(t)$, and the angular acceleration (or deceleration) of the motor shaft, ε_{d}, this concept of the single-input, single-output (SISO) control system is inadequate here.

DOI 10.2478/ama-2023-0006

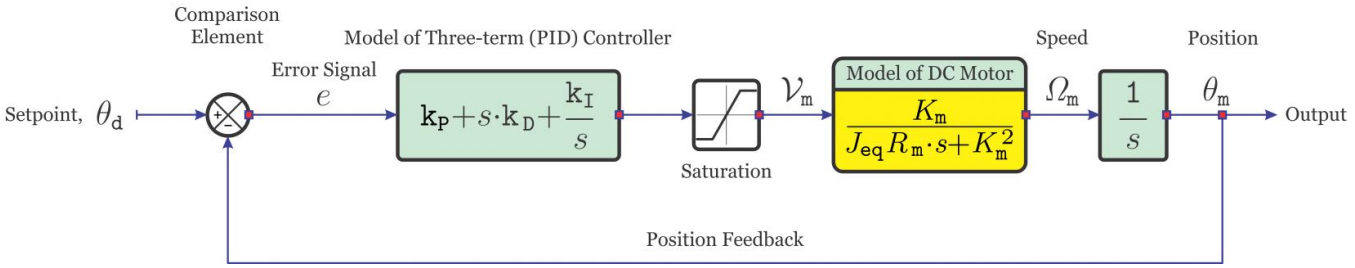

Fig. 2. Schematic of a closed-loop control system for the DC motor with PID controller. PID, proportional-integral-derivative

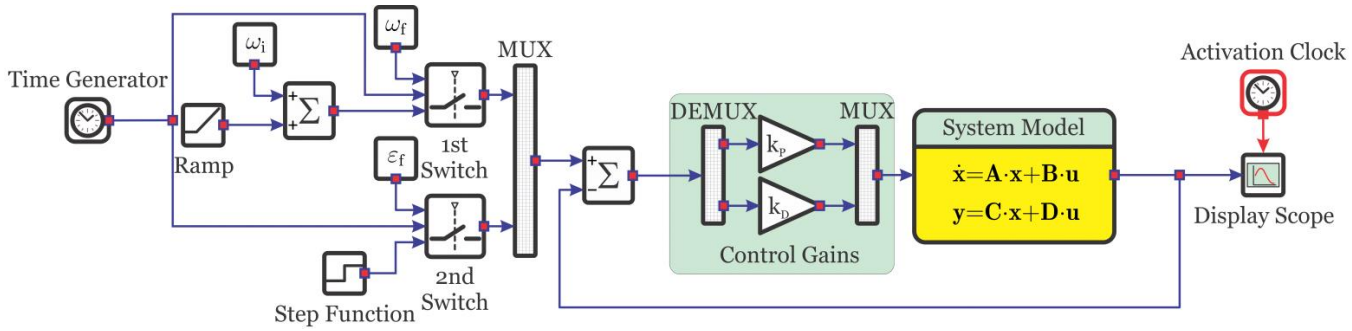

Fig. 3. Conceptual design configuration for the state-space PD feedback control. PD, proportional-derivative

Given the transfer function of the SISO system, $\Omega_m(s)/\mathcal{V}_m(s)$, it can be obtained from its multiple input-output (MIMO) state-space representations [22, 23], which is represented by the following equations:

$$\dot{\mathbf{x}}(t) = \mathbf{A}\cdot\mathbf{x}(t) + \mathbf{B}\cdot\mathbf{u}(t)\,, \tag{6}$$

$$\mathbf{y}(t) = \mathbf{C}\cdot\mathbf{x}(t) + \mathbf{D}\cdot\mathbf{u}(t)\,, \tag{7}$$

for $t \geq t_0$ and initial conditions $\mathbf{x}(t_0)$, where $\mathbf{A}$, $\mathbf{B}$, $\mathbf{C}$, and $\mathbf{D}$ are the system, input, output, and feedforward matrixes, respectively. In Eqs (6) and (7), $\mathbf{x}(t)$ is the state vector, $\dot{\mathbf{x}}(t)$ is the derivative of the state vector to time, $\mathbf{y}(t)$ is the output vector, and $\mathbf{u}(t)$ is the input (or control) vector. Eq. (6) is called the state differential equation, and Eq. (7) is the output equation.

Using Eq. (5), the transfer function of the DC motor can be converted to the state-space representation as follows

$$\begin{Bmatrix}\dot{\omega}(t)\\ \dot{\varepsilon}(t)\end{Bmatrix} = \begin{bmatrix}\frac{-K_m^2}{J_{eq}R_m} & 0\\ 0 & \frac{-K_m^2}{J_{eq}R_m}\end{bmatrix}\begin{Bmatrix}\omega(t)\\ \varepsilon(t)\end{Bmatrix} + \begin{bmatrix}\frac{K_m}{J_{eq}R_m} & 0\\ 0 & \frac{K_m}{J_{eq}R_m}\end{bmatrix}\begin{Bmatrix}v_m(t)\\ \dot{v}_m(t)\end{Bmatrix}, \tag{8}$$

$$\begin{Bmatrix}\omega(t)\\ \varepsilon(t)\end{Bmatrix} = \begin{bmatrix}1 & 0\\ 0 & 1\end{bmatrix}\begin{Bmatrix}\omega(t)\\ \varepsilon(t)\end{Bmatrix}. \tag{9}$$

After coupling with a proportional- derivative (PD) compensator, as shown in Fig. 3, the above model creates a control system that meets the design assumptions regarding the possibility of simultaneous control of the variable linearly angular velocity of the electric motor shaft, $\omega(t)$, for a predetermined constant angular acceleration (or deceleration), $\varepsilon(t)$. In the block diagram performed by Xcos/Scilab software of Fig. 3, ε_f stands for the constant acceleration (or deceleration) in the assumed period, and ω_i and ω_f stand for the initial and final velocities, respectively. In Fig. 3, $k_P = 100$ and $k_D = 10$ denotes the proportional and derivative gains, respectively.

4. COMPUTATIONAL RESULTS

The new energy recovery hybrid system with flywheels can use various operation modes listed in Section 2. Of these five strategies, let's look at the second one, i.e., 'flywheel energy storage system alone traction or alone regenerative braking'.

For computer simulations, parameters of a typical high-speed railway multiple unit train, i.e., CRH380A, are selected from Appendix A of [24]. The maximum operating speed of the train CRH380A can be up to 380 km / h. However, its regular operating speed is 350 km / h.

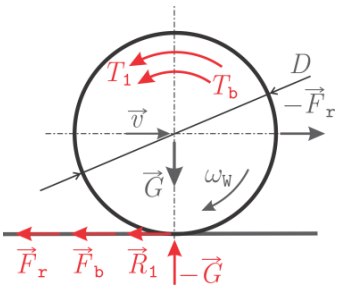

Fig. 4. Forces acting on a rotating wheel during braking

The emergency braking deceleration of some trains reaches 1.4 m/s2, and the standard braking deceleration is 1.1 m/s2. However, according to data in Table 1 presented in [25], the vehicle Sheffield Supertram (Siemens-Düwag) can brake with a deceleration of 3 m/s2 using emergency track brakes. But their use carries a high risk of passenger injury.

sciendo
DOI 10.2478/ama-2023-0006
acta mechanica et automatica, vol.17 no.1 (2023)
Special Issue "Machine Modeling and Simulations 2022"

Tab. 1. Example maximum accelerations for railway vehicles in Great Britain

Vehicle	Maximum acceleration (m/s²)		
	Traction	Service brakes	Emergency brakes
Class 390 Pendolino (intercity EMU)	0.37	0.88	1.18
Class 156 Super Sprinter (regional DMU)	0.75	0.7–0.8	0.7–0.8
Class 323 (suburban EMU)	0.99	0.88	1.18
London Underground 1992 tube stock	1.3	1.15	1.4
Tyne and Wear Metrocar	1.0	1.15	2.1 (*)
Manchester tram (Ansaldo T-68)	1.3	1.3	2.6 (*)
Sheffield Supertram (Siemens-Düwag)	1.3	1.5	3.0 (*)
Croydon tram (Bombardier FLEXITY)	1.2	1.3	2.73 (*)
Nottingham tram (Bombardier)	1.2	1.4	2.5 (*)

(*) As experience has shown, emergency track brakes are used as a last resort because their use carries a high risk of passenger injury.

The distribution of the forces acting on the braked wheel is depicted in Fig. 4. The wheel is subject to the following forces:

- the vertical forces $\vec{G}$ and $-\vec{G}$, considered in the cases of load-bearing and traction wheels,
- the resisting torque T_1, corresponding to the resistance $\vec{R}_1$,
- the braking torque $T_\mathrm{b} = F_\mathrm{b} \cdot \mathrm{D}/2$ (The overall reaction of the ground on the wheel is thus given by the resistance force $\vec{F}_\mathrm{r} = \vec{F}_\mathrm{b} + \vec{R}_1$),
- the horizontal force $-\vec{F}_\mathrm{r}$ applied to the spindle in the direction of motion, which is equal in magnitude to the ground reaction $\vec{F}_\mathrm{r}$.

Given that all driving and load-bearing wheelsets of the train are always braked, for adhesion conditions to apply, it is necessary that

$$F_\mathrm{b} \leq f(v) \cdot G\,, \tag{10}$$

where $f(v)$ is the coefficient of friction between the shoe and the rail, which depends on train speed, v.

Example 1: Regenerative braking of the multiple unit train from a speed of 50–0 m/s (all wheels at each bogie are braked in a regenerative manner with the train deceleration, aD = 1 m/s2)

In braking a train, the braking forces have to be applied to the wheels rapidly, systematically, and under control to prevent derailments. The braking operation should not be damaging to the train and its passengers. Under normal conditions, during braking, efforts should be taken to avoid any discomfort to the passengers, and if at all, it should be kept to the barest minimum.

The brake time is $t = V_0/a \cdot t$ = 50 s, and the brake distance $s = V_0 \cdot t - ½ \cdot a_\mathrm{D} \cdot t^2$ = 1250 m. Given that $\mathrm{m_{CAR}}$= 52362 kg, the total brake force per one car $F_\mathrm{b} = \mathrm{m_{CAR}} \cdot a$ = 52362 N, and the brake energy, $W_\mathrm{b} = F_\mathrm{b} \cdot s$ = 65452500 J. Because of the small moment of the inertia of the car wheels compared to the flywheels, the contribution of the wheel's change of energy is not significant. The wheel radius is $\mathrm{r_{wheel}}$ = 0.43 m and the moment of the inertia of both the same flywheels is $\mathrm{J_{FW}}$ = 5 kg·m2. The initial speed of the flywheels is ω_FW= 0 rad/s. Furthermore, the stored kinetic energy in both the flywheels is E_K = 65452500 J. Fig. 5 shows how the angular velocities of the ring, sun gear, and planet carrier of the first differential transmission are changed during braking. Fig. 6 shows the implementation of planet carrier control by the FAULHABER DC servo motor with an integrated motion controller during braking.

The torque values are as follows: $\mathrm{M_C^{(1)}} \approx 0$ N·m, $\mathrm{M_R^{(1)}}$ = 1333.1 N·m and $\mathrm{M_S^{(1)}}$ = -1536 N·m. The ratio of the second planetary gear is constant and equals $\omega_\mathrm{S}^{(2)}/\omega_\mathrm{C}^{(2)}$ = 3.5333.

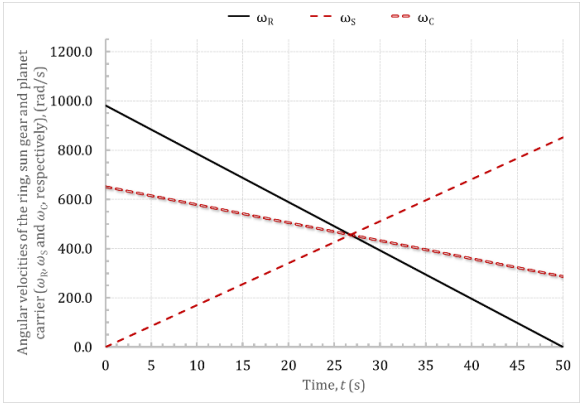

Fig. 5. Changes in the angular velocities of the ring, sun gear, and planet carrier during braking (Example 1)

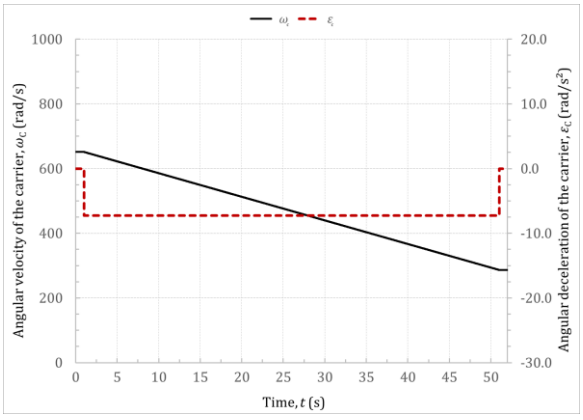

Fig. 6. Course of planet carrier control by the electric motor MG during braking (Example 1)

Example 2: Regenerative emergency braking of the multiple unit train from a speed of 50–0 m/s (all wheels at each bogie are braked in a regenerative manner with the train deceleration, aD = 3 m/s2)

DOI 10.2478/ama-2023-0006

The brake time is $t = V_0/a \cdot t$ = 16.67 s, and the brake distance $s = V_0 \cdot t - ½ \cdot a_D \cdot t^2$ = 416.67 m. The total brake force per one car $F_b = m_{CAR} \cdot a$ = 157084.74 N, and the brake energy, $W_b = F_b \cdot s$ = 65452500 J. The initial speed of the flywheels is ω_{FW} = 0 rad/s. Furthermore, the stored kinetic energy in both the flywheels is E_K = 65452500 J. Fig. 7 shows how the angular velocities of the ring, sun gear, and planet carrier have changed during braking. Fig. 8 shows the implementation of planet carrier control by the FAULHABER DC servo motor during braking.

The torque values are as follows: $M_C^{(1)} \approx 0$ N·m, $M_R^{(1)}$ = 3999.4 N·m and $M_S^{(1)}$ = -4607.9 N·m. The ratio of the second planetary gear is the same as in the previous example and equals $\omega_S^{(2)}/\omega_C^{(2)}$ = 3.5333.

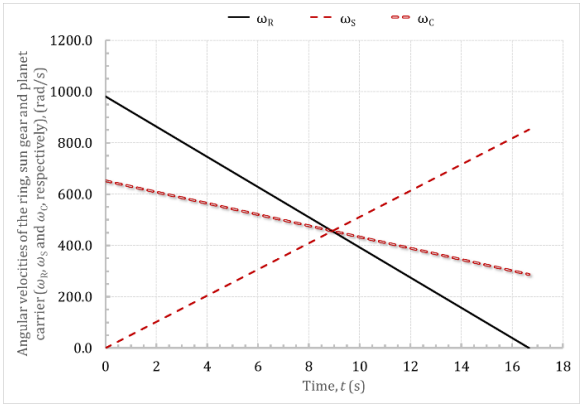

Fig. 7. Changes in the angular velocities of the ring, sun gear, and planet carrier during braking (Example 2)

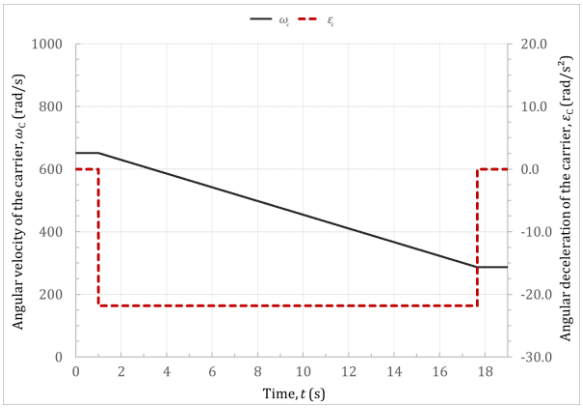

Fig. 8. Course of planet carrier control by the electric motor MG during braking (Example 2)

Example 3: Acceleration of the multiple unit train using only the energy stored in the flywheels moving from a speed of 0–50 m/s (the train acceleration, a = 1 m/s2)

The accelerating time is t = 50 s, and the traveled distance $s = ½ \cdot a \cdot t^2$ = 1250 m. The consumed kinetic energy from both the flywheels is E_K = 65452500 J. Fig. 9 shows how the angular velocities of the ring, sun gear, and planet carrier have changed during acceleration. Fig. 10 shows the implementation of planet carrier control by the FAULHABER DC servo motor during acceleration.

The torque values are as follows: $M_C^{(1)} \approx 0$ N·m, $M_S^{(1)}$ = 1536 N·m and $M_R^{(1)}$ = -1333.1 N·m. The ratio of the second planetary gear is also the same as in the previous example and equals $\omega_S^{(2)}/\omega_C^{(2)}$ = 3.5333.

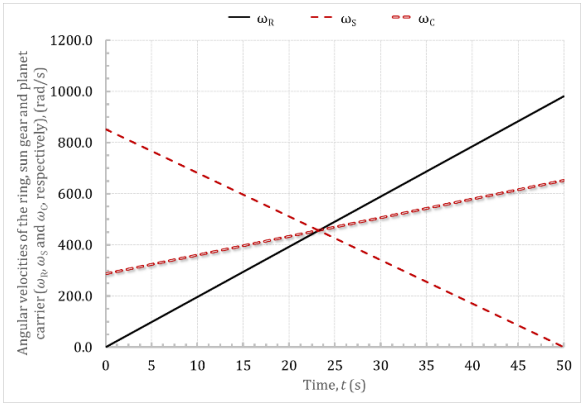

Fig. 9. Changes in the angular velocities of the ring, sun gear, and planet carrier during accelerating (Example 3)

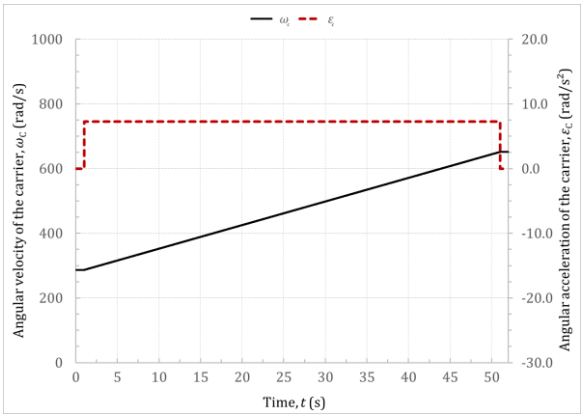

Fig. 10. Course of planet carrier control by the electric motor MG during accelerating (Example 3)

5. CONCLUSIONS

The article describes the new concept of a regenerative braking system based on flywheels, which gives a chance to introduce a more effective solution than the previously known ones. The new mechanical hybrid kinetic energy recovery system is designed under the design process of mechatronic systems. The proposed system uses new innovative, continuously variable transmission to discharge and charge the 'mechanical' batteries. This innovative transmission method offers the opportunity to obtain more desirable energy savings than before during the regenerative braking of electric multi-unit trains.

It is easy to notice that the use of a mechatronic approach during designing a new energy recovery hybrid system with flywheels significantly simplified the mechanical structure of this system. The control system of the new regenerative braking method is less complicated even compared to the control of continuously variable toroidal gears. It is an additional advantage of this solution.

The proposed system provides the ability of rail vehicles to reuse braking energy which is not lost but stored in the flywheels. However, as it has been established for railway vehicles operating at speeds up to 200 km/h, about 40% of the energy is consumed for traction (i.e., lost during variation of the kinetic energy of vehicles). Another 40% of the energy is spent by natural oscillations of the running gear and their interconnections between cars (see [26, 27]). Of the remaining 20%, 10% is consumed to overcome the frictional forces in the systems and components of railway vehicles and the interaction forces between wheels and rails, and the remainder of 10% is used to overcome air resistance.

REFERENCES

1. Spiryagin M, Cole C, Sun YQ, McClanachan M, Spiryagin V, McSweeney T. Design and simulation of rail vehicles. Boca Raton: CRC press; 2014.
2. Latto L. Regenerative braking systems in rail applications [Internet]. 2014 [cited 2022 June 20]. Available from: https://connectorsupplier.com/regenerative-braking-systems-rail-applications/
3. Kapetanović M, Vajihi M, Goverde RM. Analysis of hybrid and plug-In hybrid alternative propulsion systems for regional diesel-electric multiple unit trains. Energies. 2021; 14(18): 5920. Available from: https://doi.org/10.3390/en14185920
4. Duffner F, Mauler L, Wentker M, Leker J, Winter M. Large-scale automotive battery cell manufacturing: Analyzing strategic and operational effects on manufacturing costs. International Journal of Production Economics. 2021; 232: 107982. Available from: https://doi.org/10.1016/j.ijpe.2020.107982
5. Şahin Y. Recent progress in processing of tungsten heavy alloys. Journal of Powder Technology. 2014; Hindawi Publishing Corporation. Article ID 764306. Available from: http: //dx.doi.org /10.1155/ 2014/764306
6. Morant S. Flywheel technology generates energy efficiencies for metros. International Railway Journal [Internet]. 2017 [cited 2022 June 20]. Available from: https://www.railjournal.com/in_depth/ flywheel-technology-generates-energy-efficiencies-for- metros/
7. Khodaparastan M, Mohamed A. Flywheel vs. supercapacitor as wayside energy storage for electric rail transit systems. Inventions. 2019; 4(4): 62.
8. Qu X, Tian L, Li J, Lou C, Jiang T. Research on charging and discharging strategies of regenerative braking energy recovery system for metro flywheel. In: 3rd Asia energy and electrical engineering symposium (AEEES). IEEE. 2021: 1087-1095.
9. Meishner F, Sauer DU. Wayside energy recovery systems in DC urban railway grids. ETransportation. 2019; 1: 100001.
10. VYCON. Vycon - the proven flywheel energy storage system for rail [Internet]. 2017 [cited 2022 June 20]. Available from: https://vyconenergy.com/2017/03/13/vycon-showcases-flywheel-energy-storage-system-for-metro-rail-power-regeneration-at-asia-pacific-rail-expo/
11. Read M. Flywheel energy storage systems for rail. Doctoral dissertation. London: Imperial College; 2011.
12. Zhang JW, Wang YH, Liu GC, Tian GZ. A review of control strategies for flywheel energy storage system and a case study with matrix converter. Energy Reports. 2022; 8: 3948-3963.
13. Wu Q, Li Y, Dan P. Optimization of urban rail transit station spacing for minimizing passenger travel time. Journal of Rail Transport Planning & Management. 2022; 22: 100317. Available from: https://doi.org/ 10.1016/j.jrtpm.2022.100317
14. Brenna M, Foiadelli F, Zaninelli D. Electrical railway transportation systems. Hoboken, New Jersey: Wiley; 2018.
15. Sardar A, Dey RK, Muttana SB. A deep dive into kinetic energy recovery systems—Part 1. Auto Tech Review. 2015; 4(6): 20-25.
16. Sardar A, Dey RK, Muttana SB. A deep dive into kinetic energy recovery systems—Part 2. Auto Tech Review. 2015; 4(7): 20-24.
17. Faulhaber. DC-Motors with integrated Electronics. Technical information [Internet]. 2022 [cited 2022 June 20]. Available from: www.faulhaber-group.com
18. Arnaudo K, Karaivanov DP. Planetary gear trains. Boca Raton: CRC Press; 2019.
19. Machowski J, Lubosny Z, Bialek JW, Bumby JR. Power system dynamics: stability and control. Hoboken: Wiley; 2020.
20. Emadi, A. (Ed.). Handbook of automotive power electronics and motor drives. Boca Raton: CRC press; 2017.
21. Teach tough concepts: Closed-loop control with LabVIEW and a DC motor [Internet]. 2020 [cited 2022 June 20]. Available from: https: //knowledge.ni.com/KnowledgeArticleDetails?id=kA03q000000YHx8CAG&l=en-US
22. Dorf RC, Bishop RH. Modern control systems. 14th ed. Harlow: Pearson Education; 2022.
23. Jackiewicz J. Optimal control of automotive multivariable dynamical systems. In: Awrejcewicz J, editor. Dynamical systems theory and applications. Cham: Springer; 2017. p. 151–168.
24. Zhai W. Vehicle–track coupled dynamics: theory and applications. Singapore: Springer; 2020.
25. Powell, JP, Palacín R. Passenger stability within moving railway vehicles: Limits on maximum longitudinal acceleration.Urban Rail Transit. 2015; 1(2): 95-103.
26. Jackiewicz J. Coupler force reduction method for multiple-unit trains using a new hierarchical control system. Railway Engineering Science. 2021; 29: 163-182. Available from: https: //link.springer.com/article/ 10.1007/s40534-021-00239-w
27. Jackiewicz, J. Modeling the longitudinal dynamics of electric multiple units with Xcos/Scilab software. In: IOP conference series: Materials science and engineering. 2021; 1199(1): 012066. Available from: https://iopscience.iop.org/article/ 10.1088/1757-899X/1199/1/012066/meta

Jacek Jackieiwcz: https://orcid.org/0000-0001-7284-7639